Opt Quant Electron
DOI 10.1007/s11082-009-9288-z

Improved Dirichlet-to-Neumann map method for modeling extended photonic crystal devices

Zhen Hu · Ya Yan Lu

Received: 20 August 2008 / Accepted: 4 March 2009

Abstract A typical photonic crystal (PhC) device has only a small number of distinct unit cells. The Dirichlet-to-Neumann (DtN) map of a unit cell is an operator that maps the wave field to its normal derivative on the boundary of the cell. Based on the DtN maps of the unit cells, a PhC device can be efficiently analyzed by solving the wave field only on edges of the unit cells. In this paper, the DtN map method is further improved by an operator marching method assuming that a main propagation direction can be identified in at least part of the device. A Bloch mode expansion method is also developed for structures exhibiting partial periodicity. Both methods are formulated on a set of curves for maximum flexibility. Numerical examples are used to illustrate the efficiency of the improved DtN map method.

Keywords Photonic crystal · Numerical method · Dirichlet-to-Neumann map · Operator marching · Bloch mode expansion

1 Introduction

In recent years, many photonic components and devices have been designed using photonic crystals (Joannopoulos et al. 1995) for various applications, for example, in integrated optics. One of the most important properties of a photonic crystal (PhC) is the existence of bandgaps. For frequencies in a bandgap, microcavities and waveguides can be developed by introducing point and line defects and they can be further combined to produce various components and devices with many different functions. Numerical simulations are essential to the design and optimization of these PhC devices. Unlike the band structure problem for a perfectly periodic

Z. Hu
Joint Advanced Research Center of University of Science and Technology of China and City University of Hong Kong, Suzhou, Jiangsu, China

Z. Hu
Department of Mathematics, University of Science and Technology of China, Hefei, Anhui, China

Z. Hu · Y. Y. Lu (✉)
Department of Mathematics, City University of Hong Kong, Kowloon, Hong Kong
e-mail: mayylu@cityu.edu.hk

Published online: 21 March 2009

and infinite PhC, a PhC device has to be analyzed in a large computation domain covering many unit cells using proper boundary conditions.

Many authors used the finite-difference time-domain (FDTD) method to simulate PhC devices. Although FDTD is relatively easy to implement, it usually requires extensive computer resources and produces solutions with limited accuracy. On the other hand, standard finite element or finite difference methods used in the frequency domain, give rise to large indefinite complex and non-Hermitian systems that are difficult to solve. However, in the frequency domain, special and more efficient numerical methods can be developed to take advantage of special geometric features of the PhC devices. For ideal two-dimensional (2D) PhCs composed of infinitely long and parallel circular cylinders (rods or air-holes), the multipole method (Felbacq et al. 1994; Yonekura et al. 1999; Martin 2006) based on cylindrical wave expansions around each cylinder is particularly efficient. If a main propagation direction can be identified for the PhC device, the scattering matrix method (McPhedran et al. 1999; Yasumoto et al. 2004) can be used. It allows one to solve the original boundary value problem of the PhC device by marching the scattering matrices from one side of the structure to another. If there is a partial periodicity along the main propagation direction, a further speed-up is possible by using a recursive-doubling procedure or Bloch mode expansions (White et al. 2004) in connection with the scattering matrices.

In an earlier paper (Hu and Lu 2008), we developed a Dirichlet-to-Neumann (DtN) map method for analyzing general 2D PhC devices in an infinite background PhC. For a unit cell, the DtN map is an operator that maps the wave field to its normal derivative on the boundary of the cell, and it can often be approximated by a small matrix. The DtN maps have been used to develop efficient numerical methods for computing transmission and reflection spectra of finite PhCs (Huang and Lu 2006, 2007; Li and Lu 2007; Wu and Lu 2008) and band structures of infinite PhCs (Yuan and Lu 2006, 2007; Yuan et al. 2008). In Hu and Lu (2008), we considered arbitrary PhC devices connected by a few PhC waveguides that extend to infinity. For such a device, the DtN maps of the regular and defect unit cells allow us to avoid further calculations inside the unit cells and set up a linear system on the edges of the unit cells only. To obtain a finite computation domain, we developed rigorous boundary conditions to truncate semi-infinite PhC waveguides (Hu and Lu 2008). Compared with the multipole method, the DtN map method is less general since it relies on the underlying lattice structure of the PhC, but it is more efficient, because it gives rise to linear systems with sparse coefficient matrices.

In this paper, we develop an improved DtN map method by incorporating an operator marching (OM) method for devices where a main propagation direction can be identified and Bloch mode expansions for structures with partial periodicity along the main propagation direction. Similar to the scattering matrix method, the OM method marches a pair of operators from one end of the structure to another. It works on the wave fields directly, rather than on the coefficients in a plane wave or other eigenmode expansion. It is natural to use the OM method with the DtN map method, since both methods work on the wave fields. Similarly, we develop a version of the Bloch mode expansion method using the wave fields directly. We illustrate the improved DtN map method using the Mach–Zehnder interferometers considered in Fujisawa and Koshiba (2006).

2 Basic DtN map method

For ideal 2D problems where the structure is z-invariant and the light waves propagate in the xy plane, the governing equation is

$$\rho \frac{\partial}{\partial x}\left(\frac{1}{\rho}\frac{\partial u}{\partial x}\right) + \rho \frac{\partial}{\partial y}\left(\frac{1}{\rho}\frac{\partial u}{\partial y}\right) + k_0^2 n^2 u = 0, \tag{1}$$

where k_0 is the free space wavenumber, $n = n(\mathbf{x})$ is the refractive index and $\mathbf{x} = (x, y)$. For the E polarization, u is the z component of the electric field and $\rho = 1$. For the H polarization, u is the z component of the magnetic field and $\rho = n^2$.

We consider a PhC device in an infinite background PhC composed of certain arrangement of defect unit cells and a few PhC waveguides that extend to infinity. Assuming that the device operates at a frequency in a bandgap, the DtN map method developed in Hu and Lu (2008) involves the following steps:

1. calculate the DtN maps for all distinct unit cells;
2. truncate the domain following the edges of the unit cells;
3. find boundary conditions on those segments of the boundary that terminate PhC waveguides:
   (a) find the DtN map of the supercell for the PhC waveguide,
   (b) find the Bloch modes of the PhC waveguide,
   (c) identify the propagation direction for the propagating Bloch modes,
   (d) define the boundary condition using the Bloch modes;
4. set up equations for all edges in the truncated domain;
5. solve the linear system for the wave field on all these edges;
6. re-construct the wave field inside the unit cells if needed.

The DtN map of a unit cell S is the operator Λ such that

$$\Lambda\, u|_{\partial S} = \left.\frac{\partial u}{\partial \nu}\right|_{\partial S} \tag{2}$$

where ∂S is the boundary of S, ν is a unit normal vector of ∂S and u is an arbitrary solution of Eq. 1. In practice, we find a matrix approximation for the operator Λ by assuming that the general solution of Eq. 1 in S can be written as a linear combination of special solutions and the condition (2) is strictly valid at some collocation points on ∂S. For unit cells containing circular cylinders, we can use the cylindrical waves as the special solutions (Huang and Lu 2006; Yuan and Lu 2006). If the cylinder has a general cross section, the special solutions can be obtained by solving a boundary integral equation (Yuan et al. 2008). If the unit cell contains more than one circular cylinders, we can use the multipole method to find the special solutions (Li and Lu 2007). For Step 2, the boundary of the truncated domain is divided into a few segments. For each PhC waveguide that extends to infinity, we have a segment that truncate this waveguide and set up a boundary condition on that segment. The wave field is taken to be zero on other parts of the boundary which are sufficiently far away from the defect unit cells. Step 3 involves a few sub-steps. A supercell of a PhC waveguide covers one period in the propagation direction and it contains a finite number of unit cells, since the transverse direction is truncated. The DtN map of the supercell can be easily obtained by merging the DtN maps of the unit cells, and it gives rise to an eigenvalue problem for the Bloch modes (Huang et al. 2007). The propagation direction of a propagating Bloch mode can be identified by calculating its average power flux. On a common edge of two neighboring unit cells in the truncated domain, we can establish an equation by comparing the normal derivative of the field obtained from two different sides of the edge using the DtN maps of these two unit cells. For an edge on a segment of the boundary that terminates a PhC waveguide, we can again establish an equation by comparing the normal derivative of the field obtained from the boundary condition or the DtN map of the relevant unit cell. These equations give rise

to a linear system for the wave field on all edges in the truncated domain. Notice that the coefficient matrix of this linear system is sparse, since the equation on an interior edge is only related to the edges of the two neighboring unit cells. This is an important advantage of the DtN map method in comparison with the multipole method. In the multipole method, the linear system for coefficients of the cylindrical wave expansions around the cylinders has a dense coefficient matrix.

In the DtN map method, the number of unknowns in the final linear system is 6 to 15 times the number of unit cells, since we typically use 3 to 5 collocation points on each edge. For many structures, such as waveguide bends and branches, the DtN map method developed in Hu and Lu (2008) is sufficient, since the number of unit cells in the truncated domain is not very large. For more complicated PhC devices, such as the Mach–Zehnder interferometers studied in Fujisawa and Koshiba (2006), there can be several thousands of unit cells in the truncated domain, even when the rigorous boundary conditions for terminating PhC waveguides are used. Since the coefficient matrix in the DtN map method is sparse, the linear system with several tens of thousands unknowns is still tractable. Nevertheless, it is desirable to develop a more efficient method, since we typically have to analyze a PhC devices for many different frequencies and for many different geometric parameters. For this reason, we develop an improved DtN map method in the following sections by incorporating operator marching (OM) and Bloch mode expansion techniques.

3 Operator marching scheme

For large PhC devices, it is often possible to identify a direction along which the wave field mainly propagates forward and backward. This is not always possible for the entire structure, since the device may be connected by a few waveguides that extend to three or more different directions at infinity. However, even when such a main propagation direction can only be found in part of the structure, it is a useful feature that can be exploited by techniques developed for optical waveguides. The operator marching (OM) method was originally developed for acoustic waveguides, it has been applied to analyze piecewise uniform waveguides and finite PhCs (Huang and Lu 2006, 2007; Wu and Lu 2008). The recent version developed in Wu and Lu (2008) has more geometric flexibility than competing techniques such as the scattering matrix method.

We consider the Helmholtz equation (1) in the domain Ω depicted in Fig. 1. The boundary of Ω consists of four segments: Γ_{top} on the top, Γ_{bot} at the bottom, Γ_m to the left and Γ_0 to the right. For the PhC devices that we are considering in this paper, Γ_0 and Γ_m could be the segment that terminate semi-infinite PhC waveguides, Γ_{top} and Γ_{bot} are boundary segments

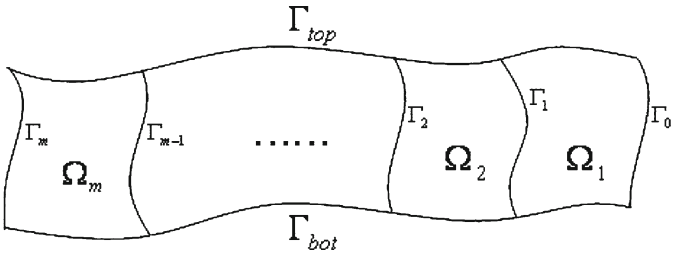

Fig. 1 The geometry for operator marching method

that truncate the infinite background PhC. Furthermore, we assume that an incident wave is given in the waveguide to the left of Γ_m and there are only outgoing waves in the waveguide to the right of Γ_0. Following Step 3 of the DtN map method outlined in Sect. 2, we have the following boundary conditions:

$$u(\mathbf{x}) = 0, \quad \mathbf{x} \in \Gamma_{top}, \quad \mathbf{x} \in \Gamma_{bot}, \tag{3}$$

$$\frac{\partial u(\mathbf{x})}{\partial \nu(\mathbf{x})} = \mathcal{L}_0^+ u(\mathbf{x}), \quad \mathbf{x} \in \Gamma_0^+, \tag{4}$$

$$\frac{\partial u(\mathbf{x})}{\partial \nu(\mathbf{x})} = \mathcal{L}_m^- u(\mathbf{x}) + f(\mathbf{x}), \quad \mathbf{x} \in \Gamma_m^-, \tag{5}$$

where $\nu = \nu(\mathbf{x})$ is a unit normal vector of Γ_0 or Γ_m, $\mathcal{L}_0^+$ and $\mathcal{L}_m^-$ are operators that act on functions defined on Γ_0 and Γ_m, respectively. To include possible dielectric interfaces on Γ_0 and Γ_m, which give rise to discontinuities of $\partial u/\partial \nu$ in the H polarization, the boundary conditions (4) and (5) are imposed from the outside of the domain Ω. That is, Γ_0^+ and Γ_m^- indicate the limits to Γ_0 and Γ_m from the right and left sides, respectively. The boundary condition (5) is inhomogeneous, where f is a function related to the given incident wave. Many examples for boundary conditions (4) and (5) can be found in Hu and Lu (2008).

In the OM method, domain Ω is decomposed into sub-domains $\Omega_1, \Omega_2, \ldots, \Omega_m$ based on "vertical" curves $\Gamma_1, \Gamma_2, \ldots, \Gamma_{m-1}$ as shown in Fig. 1. On each curve Γ_j, we define two operators Q_j and Y_j by

$$Q_j u(\mathbf{x}) = \frac{\partial u}{\partial \nu}(\mathbf{x}), \quad Y_j u(\mathbf{x}) = u_0, \quad \mathbf{x} \in \Gamma_j^+, \tag{6}$$

where u is any solution of Eq. 1 satisfying (3) and (4), $\nu(\mathbf{x})$ is a unit normal vector of Γ_j at $\mathbf{x}$ and $u_0 = u|_{\Gamma_0}$. From (4) and the definition of Y_j, we have

$$Q_0 = \mathcal{L}_0^+, \quad Y_0 = I, \tag{7}$$

where I is the identity operator. If Q_m and Y_m are obtained, we can find the wave field on Γ_0 and Γ_m. From the continuity of $\rho^{-1}\partial_\nu u$, we have

$$\left.\frac{\partial u}{\partial \nu}\right|_{\Gamma_m^-} = \sigma_m \left.\frac{\partial u}{\partial \nu}\right|_{\Gamma_m^+} = \sigma_m Q_m u_m,$$

where $u_m = u|_{\Gamma_m}$, $\sigma_m = \rho_m^-/\rho_m^+$ and $\rho_m^\pm = \rho|_{\Gamma_m^\pm}$. Condition (5) then gives us

$$(\sigma_m Q_m - \mathcal{L}_m^-)u_m = f. \tag{8}$$

Finally, we can multiply Y_m to find u on Γ_0:

$$u_0 = Y_m u_m. \tag{9}$$

To march the operators from Γ_{j-1} to Γ_j, we need the reduced DtN map M_j of the domain Ω_j satisfying

$$M^{(j)} \begin{bmatrix} u_j \\ u_{j-1} \end{bmatrix} = \begin{bmatrix} M_{11}^{(j)} & M_{12}^{(j)} \\ M_{21}^{(j)} & M_{22}^{(j)} \end{bmatrix} \begin{bmatrix} u_j \\ u_{j-1} \end{bmatrix} = \begin{bmatrix} \partial_\nu u_j^+ \\ \partial_\nu u_{j-1}^- \end{bmatrix}, \tag{10}$$

where $u_j = u|_{\Gamma_j}$, $\partial_\nu u_j^+ = \partial_\nu u|_{\Gamma_j^+}$, etc. Notice that $M^{(j)}$ is defined from the interior of the domain Ω_j, thus the normal derivatives on Γ_j and Γ_{j-1} are taken from right and left, respectively. From the continuity of $\rho^{-1}\partial_\nu u$ on Γ_{j-1}, we have

$$\partial_\nu u_{j-1}^- = \sigma_{j-1} Q_{j-1} u_{j-1}, \tag{11}$$

where $\sigma_{j-1} = \rho_{j-1}^-/\rho_{j-1}^+$ and $\rho_{j-1}^\pm = \rho|_{\Gamma_{j-1}^\pm}$. If we replace $\partial_\nu u_{j-1}^-$ and $\partial_\nu u_j^+$ in (10) by $\sigma_{j-1} Q_{j-1} u_{j-1}$ and $Q_j u_j$ respectively, and eliminate u_{j-1}, we obtain the following marching formulas:

$$P = \left[\sigma_{j-1} Q_{j-1} - M_{22}^{(j)}\right]^{-1} M_{21}^{(j)}, \tag{12}$$

$$Q_j = M_{11}^{(j)} + M_{12}^{(j)} P, \tag{13}$$

$$Y_j = Y_{j-1} P. \tag{14}$$

In practice, the operators are all approximated by matrices. Since Γ_j, for $0 \le j \le m$, are curves in general, the OM method is more flexible than the scattering matrix method. The latter requires Γ_j to be a set of parallel straight lines, so that the wave field there can be expanded in plane waves or other eigenmodes. The advantage of OM for operators defined on curves was exploited to analyze interpenetrating arrays of circular cylinders in Wu and Lu (2008).

4 Bloch mode expansion

In this section, we consider partial periodic structures. More precisely, we assume that the structure is periodic between Γ_k and Γ_{k+n} along the x direction with period a, where $k \ge 0$ and $n > 0$ are integers. This implies that the curve Γ_{k+l} is a horizontal translation of Γ_k by the distance $-la$, and the sub-domain Ω_{k+l} is a horizontal translation of Ω_{k+1} by the distance $(-l+1)a$, where l is an integer satisfying $1 \le l \le n$. The top and bottom boundaries Γ_{top} and Γ_{bot} (between Γ_k and Γ_{k+n}) are also periodic in x and they do not need to be flat in general. In the following, we present a Bloch mode expansion method so that the operators Q_{k+n} and Y_{k+n} can be obtained from Q_k and Y_k directly.

First, we consider the structure between Γ_k and Γ_{k+n} as a periodic waveguide and find its Bloch modes. To do this, we make use of the reduced DtN map M, satisfying Eq. 10, of the sub-domain Ω_j for $k+1 \le j \le k+n$, where the superscript $^{(j)}$ is dropped to simplify the notation. A Bloch mode of the periodic waveguide is a solution of Eq. 1 given in the form

$$\Phi(x, y) = e^{i\beta x} \hat{\Phi}(x, y) \tag{15}$$

where $\hat{\Phi}$ is periodic in x with period a. This implies that

$$\Phi|_{\Gamma_{j-1}} = \mu \Phi|_{\Gamma_j}, \quad \left.\frac{\partial \Phi}{\partial \nu}\right|_{\Gamma_{j-1}^+} = \mu \left.\frac{\partial \Phi}{\partial \nu}\right|_{\Gamma_j^+}, \quad \mu = e^{i\beta a}. \tag{16}$$

As in Huang et al. (2007), an eigenvalue problem can be formulated for the Bloch modes using the reduced DtN map M. We have

$$\begin{bmatrix} M_{11} & -I \\ M_{21} & 0 \end{bmatrix} \begin{bmatrix} \phi \\ \phi' \end{bmatrix} = \mu \begin{bmatrix} -M_{12} & 0 \\ -M_{22} & \sigma_{j-1} \end{bmatrix} \begin{bmatrix} \phi \\ \phi' \end{bmatrix}, \tag{17}$$

where σ_{j-1} is defined after Eq. 11, M_{11}, M_{12}, M_{21} and M_{22} are the blocks of M, and

$$\phi = \Phi|_{\Gamma_j}, \quad \phi' = \left.\frac{\partial \Phi}{\partial \nu}\right|_{\Gamma_j^+}. \tag{18}$$

The eigenvalues appear in pairs, namely, if μ is an eigenvalue, so is $\mu^{-1} = e^{-i\beta a}$. We can choose β so that $|\mu| = |e^{i\beta a}| \leq 1$. Furthermore, if $|\mu| = 1$, we choose a real β so that the propagating Bloch mode has a positive average power flux in the x direction. The case $|\mu| < 1$ corresponds to an evanescent Bloch mode that decays exponentially as x is increased. Those Bloch modes corresponding to $\mu^{-1} = e^{-i\beta a}$ are denoted by $\Psi(x, y) = e^{-i\beta x}\hat{\Psi}(x, y)$, where $\hat{\Psi}$ is periodic in x.

With the Bloch modes, we can decompose the general wave field in the periodic structure as forward and backward components:

$$u = u^+ + u^-, \tag{19}$$

where u^+ is a sum of Bloch modes that propagate toward $x = +\infty$ or decay exponentially as x is increased, and u^- is the opposite. More precisely,

$$u^+(x, y) = \sum_{p=1}^{\infty} c_p\, \Phi_p(x, y) = \sum_{p=1}^{\infty} c_p\, e^{i\beta_p x}\, \hat{\Phi}_p(x, y), \tag{20}$$

$$u^-(x, y) = \sum_{p=1}^{\infty} d_p\, \Psi_p(x, y) = \sum_{p=1}^{\infty} d_p\, e^{-i\beta_p x}\, \hat{\Psi}_p(x, y), \tag{21}$$

where c_p and d_p are unknown coefficients.

Based on the Bloch mode expansion (19, 20, 21), we can define two operators $\mathcal{T}_0$ and $\mathcal{T}_1$ such that

$$\mathcal{T}_0 u_j^+ = u_{j-1}^+, \quad \mathcal{T}_1 u_{j-1}^- = u_j^-, \quad j = k+1, \ldots, k+n, \tag{22}$$

where $u_j^+ = u^+|_{\Gamma_j}$, $u_j^- = u^-|_{\Gamma_j}$, etc. Here, $\mathcal{T}_0$ is a translation operator for the wave field component u^+. It maps u^+ on Γ_j in the positive x direction by distance a to u^+ on Γ_{j-1}. Let $\Phi_p|_{\Gamma_j} = \phi_p$ as in (18), we define $\mathcal{T}_0$ as a linear operator satisfying

$$\mathcal{T}_0 \phi_p = \mu_p\, \phi_p, \quad p = 1, 2, \ldots \tag{23}$$

In practice, when the reduced DtN map M is approximated by a matrix and ϕ is approximated by a column vector, $\mathcal{T}_0$ is the matrix given by

$$\mathcal{T}_0 = \begin{bmatrix} \phi_1 & \phi_2 & \ldots \end{bmatrix} \begin{bmatrix} \mu_1 & & \\ & \mu_2 & \\ & & \ddots \end{bmatrix} \begin{bmatrix} \phi_1 & \phi_2 & \ldots \end{bmatrix}^{-1}. \tag{24}$$

Similarly, $\mathcal{T}_1$ is defined by

$$\mathcal{T}_1 \psi_p = \mu_p\, \psi_p, \quad p = 1, 2, \ldots \tag{25}$$

where $\psi_p = \Psi_p|_{\Gamma_j}$. If we apply the operators $\mathcal{T}_0$ and $\mathcal{T}_1$ repeatedly, we have

$$u_{k+l} = u_{k+l}^+ + u_{k+l}^- = \mathcal{T}_0^{n-l}\, f + \mathcal{T}_1^l\, g, \tag{26}$$

where l is any integer satisfying $0 \leq l \leq n$ and

$$f = u_{k+n}^+, \quad g = u_k^-.$$

To find the relationships between $\{Q_k, Y_k\}$ and $\{Q_{k+n}, Y_{k+n}\}$, we evaluate the normal derivatives of u on Γ_k and Γ_{k+n} using Q_k, Q_{k+n} and the reduced DtN map M in sub-domains Ω_{k+1} and Ω_{k+n}. We obtain

$$M_{21}\, u_{k+1} + M_{22}\, u_k = \sigma_k Q_k\, u_k, \tag{27}$$

$$M_{11}\, u_{k+n} + M_{12}\, u_{k+n-1} = Q_{k+n}\, u_{k+n}. \tag{28}$$

If we re-write u_k, u_{k+1}, u_{k+n-1} and u_{k+n} in terms of f and g, we first obtain

$$P = (M_{21}\mathcal{T}_1 + M_{22} - \sigma_k Q_k)^{-1}\left[(\sigma_k Q_k - M_{22})\mathcal{T}_0 - M_{21}\right]\mathcal{T}_0^{n-1} \tag{29}$$

such that $g = Pf$ and then

$$Q_{k+n} = \left[M_{11} + M_{12}\mathcal{T}_0 + (M_{11}\mathcal{T}_1 + M_{12})\mathcal{T}_1^{n-1}P\right]\left(1 + \mathcal{T}_1^n P\right)^{-1}, \tag{30}$$

$$Y_{k+n} = Y_k(\mathcal{T}_0^n + P)\left(1 + \mathcal{T}_1^n P\right)^{-1}. \tag{31}$$

The formulas above allow us to evaluate Q_{k+n} and Y_{k+n} directly from the given Q_k and Y_k. Notice that the powers of $\mathcal{T}_0$ and $\mathcal{T}_1$ are evaluated using the eigenvalue decomposition (24) by taking the powers of the eigenvalues in the diagonal matrix. The operators $\mathcal{T}_0$ and $\mathcal{T}_1$ are also used in the derivation of boundary conditions that terminate semi-infinite PhC waveguides (Hu and Lu 2008).

5 Numerical examples

To illustrate our method, we consider two examples originally analyzed by Fujisawa and Koshiba (2006). The first example is a Mach–Zehnder interferometer based on PhC waveguides where the bulk PhC is a triangular lattice of circular rods in a background dielectric medium. The refractive indices of the rods and the background medium are 3.5 and 1.5, respectively, and the radius of the rods is $0.25a$ where a is the lattice constant. For the E polarization, the bulk PhC has a bandgap given by $0.235 < \omega a/(2\pi c) < 0.315$. The PhC waveguides are created by defect cells where the radius of rods is reduced to $0.15a$. A line defect gives rise to a single mode waveguide for an interval of frequencies in the bandgap Fujisawa and Koshiba (2006). As shown schematically in Fig. 2, two PhC waveguides which are parallel at infinity are brought closer in two coupling regions of length $L_c = 20a$, and these two regions are separated by the distance $L_a = 100a$. Away from the coupling regions, the two waveguides are separated by seven layers of rods. For this structure, we specify an incoming wave (the propagating mode) in the top left PhC waveguide (port 1) and calculate the reflected wave in port 1 and the transmitted waves in the other three waveguides (ports 2–4 shown in Fig. 2).

To use the DtN map method, we truncate the domain as in Fig. 2. The boundaries Γ_0, Γ_m, Γ_{top} and Γ_{bot} are not straight lines, since the domain is truncated along edges of the hexagon unit cells. For a triangular lattice, rectangle and parallelogram unit cells can also be used, but the hexagon unit cells are preferred because of their greater symmetry. The truncated domain contains $142 \times 19 = 2698$ unit cells. In our calculations, we use 5 collocation points on each edge of the unit hexagon cells. This corresponds to 30 cylindrical waves in each unit cell. For these choices, the original DtN map method (Hu and Lu 2008) gives rise to a sparse linear system for about 40000 unknowns. In the OM method, the two operators Q_j and Y_j are represented by 185×185 matrices, and they are marched from Γ_0 to Γ_m for $m = L_a + 2L_c + 2 = 142$. Here, the curve Γ_j is simply a horizontal translation of Γ_0 by $-ja$. The domain Ω_j bounded by Γ_j and Γ_{j-1} contains 19 unit cells, and its reduced DtN map $M^{(j)}$ can be easily obtained by merging the DtN maps of the unit cells as described in Huang et al. (2007). Since the structure contains a large periodic segment between the two coupling regions, we use the Bloch mode expansion method to further speed up the computation. As shown in Fig. 2, the structure is periodic in x between Γ_k and Γ_{k+n}, where $k = 21$ and $k + n = 121$.

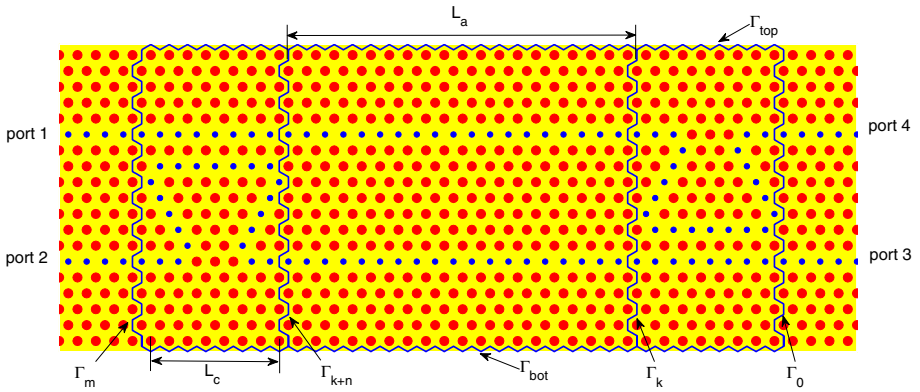

Fig. 2 Mach–Zehnder interferometer proposed in Fujisawa and Koshiba (2006) based on photonic crystal waveguides in a triangular lattice

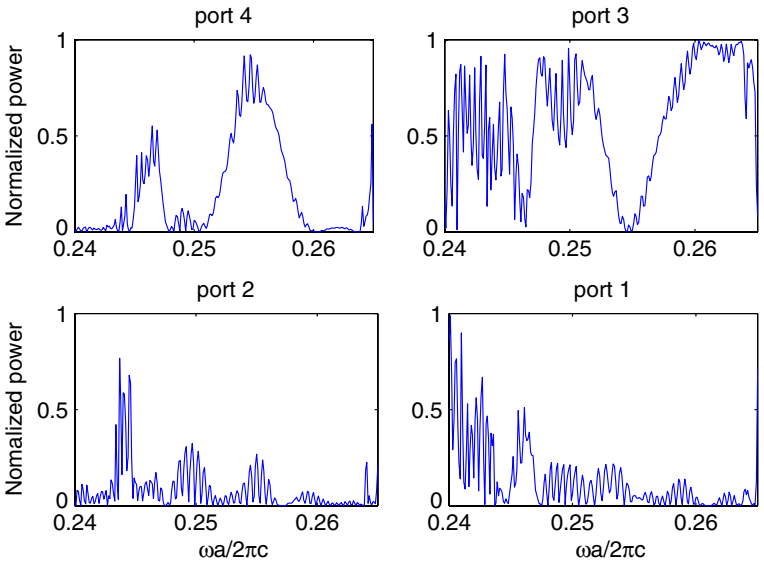

Fig. 3 Normalized output power in the four ports as functions of $\omega a/(2\pi c)$ for the Mach–Zehnder interferometer shown in Fig. 2

The structure also has two smaller periodic segments in the coupling regions, but the Bloch mode expansion method has little advantage there since the number of periods is not sufficiently large. For this example, the DtN map method with OM and Bloch mode expansion is much more efficient than the original method in (Hu and Lu 2008) and it requires less computer memory. On a personal computer with a Intel Q6600 CPU of 2.4 GHz, the simulation for one frequency requires only 8 s. Our results are presented in Fig. 3, where the normalized output power in all four ports are given as functions of $\omega a/(2\pi c)$.

The second example as shown in Fig. 4, is also a Mach–Zehnder interferometer, but the bulk PhC is a square lattice of dielectric rods in a background medium. The waveguides are also created by reducing the radius of rods in the defect unit cells. As in the first example,

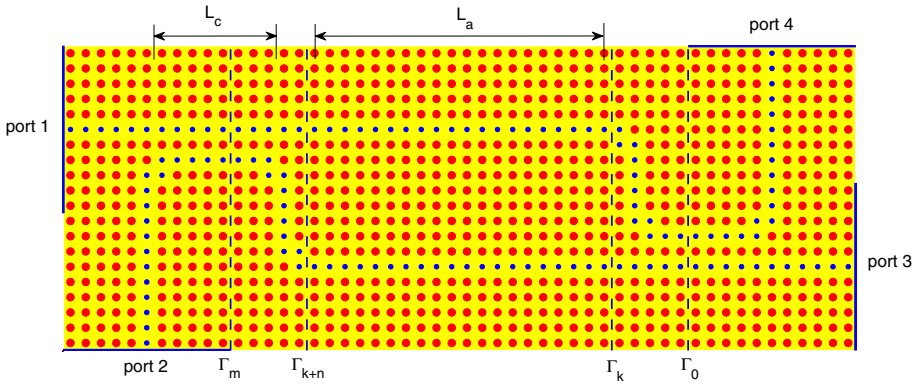

Fig. 4 Mach–Zehnder interferometer proposed in Fujisawa and Koshiba (2006) based on photonic crystal waveguides in a square lattice

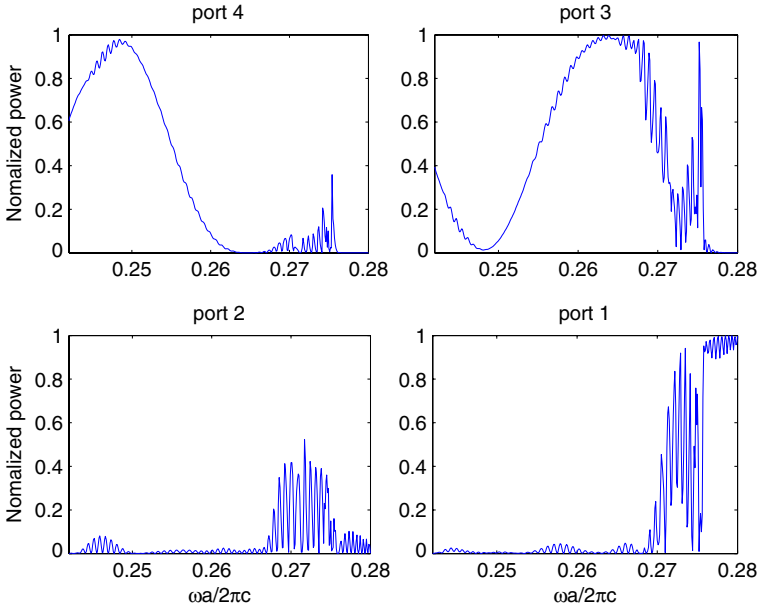

Fig. 5 Normalized output power in the four ports as a function of $\omega a/(2\pi c)$ for the Mach–Zehnder interferometer shown in Fig. 4

the refractive indices of rods and background medium are 3.5 and 1.5, respectively, and the radii of the regular and defect rods are $0.25a$ and $0.15a$, respectively. For this structure, the coupling length is $L_c = 15a$ and the length of arm is assumed to be $L_a = 130a$. As before, the incident wave is a propagating mode in the top left waveguide (port 1) and we calculate the waves that are reflected or transmitted to all four waveguides.

Since the four waveguides extend to four different directions at infinity, this example does not have a main propagation direction for the entire structure. However, the OM method can still be applied to part of the structure and Bloch mode expansion can still be used to speed up the computation. In our implementation, we truncate the domain by keeping at least

five layers of rods in directions transverse to the waveguide axes. The truncated domain is a rectangle containing $(L_a + 2L_c + 17) \times 20 = 3540$ unit cells. For each waveguide, we set up rigorous boundary conditions on a line segment of length $11a$ following the procedures established in Hu and Lu (2008). These four line segments are shown as the solid lines on the boundary of the truncated domain in Fig. 4. On other parts of the boundary, the field is assumed to be zero. If the original DtN map method is used, we set up a linear system for the wave field on all edges of the square unit cells in the truncated domain. If we use 5 collocation points on each edge, then the linear system involves about 35000 unknowns. Fortunately, we can still use the OM method between Γ_0 and Γ_m shown in Fig. 4. Here, Γ_0 and Γ_m are vertical lines with a distance of $11a$ away from the right and left edges of the truncated domain. They are chosen so that the simple zero boundary condition is valid on the top and bottom boundaries between Γ_0 and Γ_m. Let the truncated domain be divided into three regions (Regions 1, 2 and 3) from right to left by the vertical lines Γ_0 and Γ_m, the OM method can be used in Region 2 and the original DtN map method Hu and Lu (2008) must be used in Regions 1 and 3. More precisely, we solve this problem in four steps:

1. in Region 1, find Q_0 such that $\partial_x u = Q_0 u$ on Γ_0;
2. in Region 2, find Q_m and Y_m assuming $Y_0 = I$;
3. solve u in Region 3 and find u on Γ_0 by $u_0 = Y_m u_m$;
4. solve u in Region 1.

Step 1 requires a slight modification of the original DtN map method developed in Hu and Lu (2008). After setting up equations on all edges in Region 1 (without the edges of Γ_0 and the boundary edges where $u = 0$), we find a matrix that links u on all these edges with u_0. Using the DtN maps of the unit cells, we find that $\partial_x u$ on Γ_0 is related to u_0 and some nearby edges in Region 1. We can eliminate u on those nearby edges and obtain Q_0. Step 2 follows the OM method with Γ_j given as a horizontal translation of Γ_0 by $-ja$. The Bloch mode expansion method can be used between Γ_k and Γ_{k+n} shown in Fig. 4, where $k = 12$ and $k + n = 143$. Steps 3 and 4 follow the original DtN map method in Hu and Lu (2008) exactly. In Fig. 5, we show the normalized output power in the four ports for various values of the frequency. These results are obtained by the method developed in this paper using 5 collocation points on each edge of the unit cells. For each frequency, the required computing time is only 10 seconds on a personal computer with an Intel Q6600 CPU of 2.4 GHz.

6 Conclusion

In this paper, we developed an improved DtN map method for modeling large PhC devices by incorporating operator marching (OM) and Bloch mode expansion techniques. The OM method is applicable if a main propagation direction can be identified in at least part of the structure. Compared with the scattering matrix method (White et al. 2004), the OM method is more flexible because it is formulated on a set of curves: Γ_j for $0 \le j \le m$. In each step, we march two operators from one curve to another through the local DtN map $M^{(j)}$ of the domain between the two curves. The scattering matrix method is formulated on a set of parallel straight lines, because it requires splitting the wave field as forward and backward components and expanding them into plane waves. Our method is also efficient because the two operators on each curve can be approximated by relatively small matrices and the local DtN map $M^{(j)}$ can be easily calculated by merging the DtN maps of the unit cells. To take advantage of the possible periodicity of the structure along the main propagation direction, we developed a Bloch mode expansion method consistent with the marching scheme on

curves. Numerical examples involving thousands of unit cells are used to demonstrate the efficiency and flexibility of our method.

Acknowledgements This research was partially supported by a grant from the Research Grants Council of Hong Kong Special Administrative Region, China (Project No. CityU 102207).

References

Felbacq, J.D., Tayeb, C., Maystre, D.: Scattering by a random set of parallel cylinders. J. Optical Soc. Am. A **11**, 2526–2538 (1994)

Fujisawa, T., Koshiba, T.: Finite-element modeling of nonlinear Mach-Zehnder interferometers based on photonic-crystal waveguides for all-optical signal processing. J. Lightwave Technol. **24**, 617–623 (2006)

Hu Z., Lu Y.Y.: Efficient analysis of photonic crystal devices by Dirichlet-to-Neumann maps. Opt. Express **16**, 17282–17399 (2008)

Huang, Y., Lu, Y.Y.: Scattering from periodic arrays of cylinders by Dirichlet-to-Neumann maps. J. Lightwave Technol. **24**, 3448–3453 (2006)

Huang, Y., Lu, Y.Y.: Modeling photonic crystals with complex unit cells by Dirichlet-to-Neumann maps. J. Comput. Math. **25**, 337–349 (2007)

Huang, Y., Lu, Y.Y., Li, S.: Analyzing photonic crystal waveguides by Dirichlet-to-Neumann maps. J. Optical Soc. Am. B **24**, 2860–2867 (2007)

Joannopoulos, J.D., Meade, R.D., Winn, J.N.: Photonic Crystals: Molding the Flow of Light. Princeton University Press, Princeton, NJ

Li, S., Lu, Y.Y.: Multipole Dirichlet-to-Neumann map method for photonic crystals with complex unit cells. J. Optical Soc. Am. A **24**, 2438–2442 (2007)

Martin, P.A.: Multiple Scattering. Cambridge University Press, Cambridge, UK (2006)

McPhedran, R.C., Botten, L.C., Asatryan, A.A., et al.: Calculation of electromagnetic properties of regular and random arrays of metallic and dielectric cylinders. Phys. Rev. E **60**, 7614–7617 (1999)

White, T.P., Botten, L.C., de Sterke, C.M., McPhedran, R.C., Asatryan, A.A., Langtry, T.N.: Block mode scattering matrix methods for modeling exteded photonic crystal structures. Applications. Phys. Rev. E **70**, 056607 (2004)

Wu, Y., Lu, Y.Y.: Dirichlet-to-Neumann map method for analyzing interpenetrating cylinder arrays in a triangular lattice. J. Optical Soc. Am. B **25**, 1466–1473 (2008)

Yasumoto, K., Toyama, H., Kushta, T.: Accurate analysis of two-dimensional electromagnetic scattering from multilaye red periodic arrays of circular cylinders using lattice sums technique. IEEE Trans. Antennas Propag. **52**, 2603–2611 (2004)

Yonekura, J., Ikeda, M., Baba, T.: Analysis of finite 2-D photonic crystals of columns and lightwave devices using the scattering matrix method. J. Lightwave Technol. **17**, 1500–1508 (1999)

Yuan, J., Lu, Y.Y.: Photonic bandgap calculations using Dirichlet-to-Neumann maps. J. Optical Soc. Am. A **23**, 3217–3222 (2006)

Yuan, J., Lu, Y.Y.: Computing photonic band structures by Dirichlet-to-Neumann maps: the triangular lattice. Optics Commun. **273**, 114–120 (2007)

Yuan, J., Lu, Y.Y., Antoine, X.: Modeling photonic crystals by boundary integral equations and Dirichlet-to-Neumann maps. J. Comput. Phys. **227**, 4617–3629 (2008)